Vitamin B1 Based Thiazol-2-ylidene Ru(II) Complexes: Recyclable Transfer Hydrogenation Catalysts in Water

Rafet Kılınçarslan,[a*] Hayriye Tuncer,[a] Namık Özdemir [b] and Bekir Çetinkaya [c]

[a] *Pamukkale University, Faculty of Science, Department of Chemistry, 20160, Denizli, Turkey*
[b] *Ondokuz Mayıs University, Faculty of Science, Department of Physics, 55139, Samsun, Turkey*
[c] *Ege University, Faculty of Science, Department of Chemistry, 35100, Izmir, Turkey*

E-mail: rkilincarslan@pau.edu.tr

Table of Contents

General Considerations

The reactions related to air sensitive parts were performed in an atmosphere of dry argon by using a Schlenk-type flask and high vacuum-line techniques. All glassware was heated under vacuum and filled with argon to eliminate moisture and oxygen. All materials, reagents and solvents were purchased from commercial suppliers. Analytical grade solvents were dried by standard methods and distilled prior to use under argon atmosphere. NMR spectra were recorded at 297 K on a Varian Mercury AS 400 NMR instrument at 400 MHz (^{1}H), 100.56 MHz (^{13}C) NMR multiplicities are abbreviated as follows: s, singlet; d, doublet; dd, doublet of doublets; t, triplet; m, multiplet; signal. Chemical shifts (δ) are quoted as ppm downfield from $SiMe_4$ using the residual protonated solvent as an internal standard and the coupling constants J are reported in Hz. Thermo scientific TSQ quantis LC-MS/MS system was used. It was carried out using the direct infusion ESI-MS/MS method. Pump speed is 20 microliters/minute. Initial source device setting are as follows; spray voltage: 3500 V, ion transfer tube temperature: 275°C, vaporizer temperature: 75°C, sheath gas (arb): 30, aux gas (arb): 8. Melting points were found using an Electrothermal 9100. The reactions were monitored by TLC, made on silica gel plates 60 F254. The image on TLC was used with UV light. Quantitative analyses were performed by GC. (HP, Agilant-6890N on an HP-5 capillary column and equipped with a FID detector). Elemental analysis was performed by direct combustion with a Leco, CHNS-932 instrument.

Appendix A. Supplementary data

CCDC 2233948 and 2321199 contain the supplementary crystallographic data for the compounds reported in this article. These data can be obtained free of charge from The Cambridge Crystallographic Data Centre via www.ccdc.cam.ac.uk/structures.

Synthesis of [(p-cymene)RuCl(κ² C,N-{C_{NHC}-NH})]$^{+}$Cl^{-} (2)

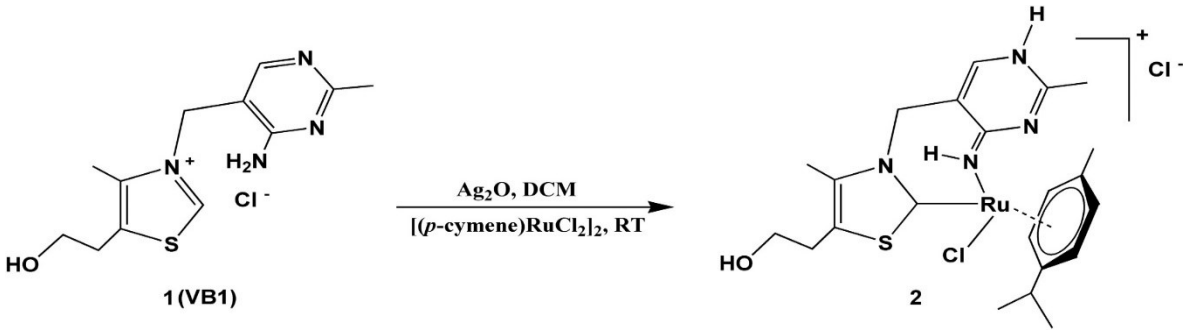

A mixture of VB1 (337.3 mg; 1.0 mmol), Ag_2O (231.7 mg; 1.0 mmol), [(*p*-cymene)$RuCl_2$]$_2$ (306.2 mg; 0.5 mmol) and 20 mL of DCM was stirred at RT under dark conditions for 48 h. After this time, DCM was evaporated in vacuo. The chilled methanol (10 mL) was added to the residue and the mixture was filtered through a pad of celite. The volume of the solution was reduced and diffusion of Et_2O into a saturated MeOH solution yielded red-brown crystals, suitable for X-ray diffraction study. The solid (479 mg, 84%). mp > 282 °C (decompose). Elemental analysis (%): calcd for $C_{22}H_{30}Cl_2N_4OSRu$: C 46.3, H 5.3, N 9.8%. Found: C 46.1, H 5.4, N 9.8. ^{1}H NMR (400 MHz, d_6-DMSO): δ = 1.17, (d, *J* = 6.80 Hz, 3H, CH_3)$_2$CH $_{cym}$), 1.20 (d, *J* = 6.80 Hz, 3H, CH_3)$_2$CH $_{cym}$), 1.99 (s, 3H, CH_3 $_{cym}$), 2.14 (s,3H, CH_3 $_{pym}$), 2.42 (s, 3H, CH_3 $_{thiaz}$), 2.65-2.71 (m, 1H, (CH$_3$)$_2$CH_{cym}), 2.80-2.83 (2H, m, CH_2CH$_2$-OH), 3.53 (q, *J* = 5.73 Hz, 2H, -CH$_2$CH_2-OH), 4.96 (t, *J* = 5.00 Hz, 1H, *H*O-CH$_2$CH$_2$), 5.19 (d, *J* = 14.8 Hz,1H, Ar-*H* $_{cym}$), 5.31 (d, *J* = 14.8 Hz, 1H, Ar-*H* $_{cym}$), 5.45 (d, 6.0 Hz, Ar-*H* $_{cym}$), 5.68 (d, *J* = 6.0 Hz, 1H, Ar-*H* $_{cym}$), 5.77 (d$_{(distorted)}$, 2H, N-CH_2), 6.24 (br s, 1H, N*H* $_{pym}$), 7.93 (s, 1H, Ar-C*H* $_{pym}$), 12.63 (br s, 1H, N*H* $_{imino}$). ^{13}C NMR (100,56 MHz, d_6-DMSO): δ = 13.4 (*C*H$_3$ $_{thiaz}$), 18.2 (*C*H$_3$ $_{cym}$), 21.0 (*C*H$_3$ $_{pym}$), 22.3, 22.8 (*C*H$_3$)$_2$CH $_{cym}$), 30.5 (CH$_3$)$_2$*C*H $_{cym}$), 30.8 (-*C*H$_2$CH$_2$-OH), 61.0 (-CH$_2$*C*H$_2$-OH), 49.0, 50.8 (Ar-*C*H $_{cym}$), 84.0, 87.1 (Ar-*C* $_{cym}$), 89.4 (d, *J* =26.3 Hz, N-*C*H$_2$), 108.2 (*C* $_{pym}$), 139.4 (*C*H $_{pym}$), 134.8, 140.7 (-*C*=*C* $_{thiaz}$), 156.5 (*C* $_{pym}$), 165.2 (*C* $_{pym}$), 212.4 (C_{NSHC}).

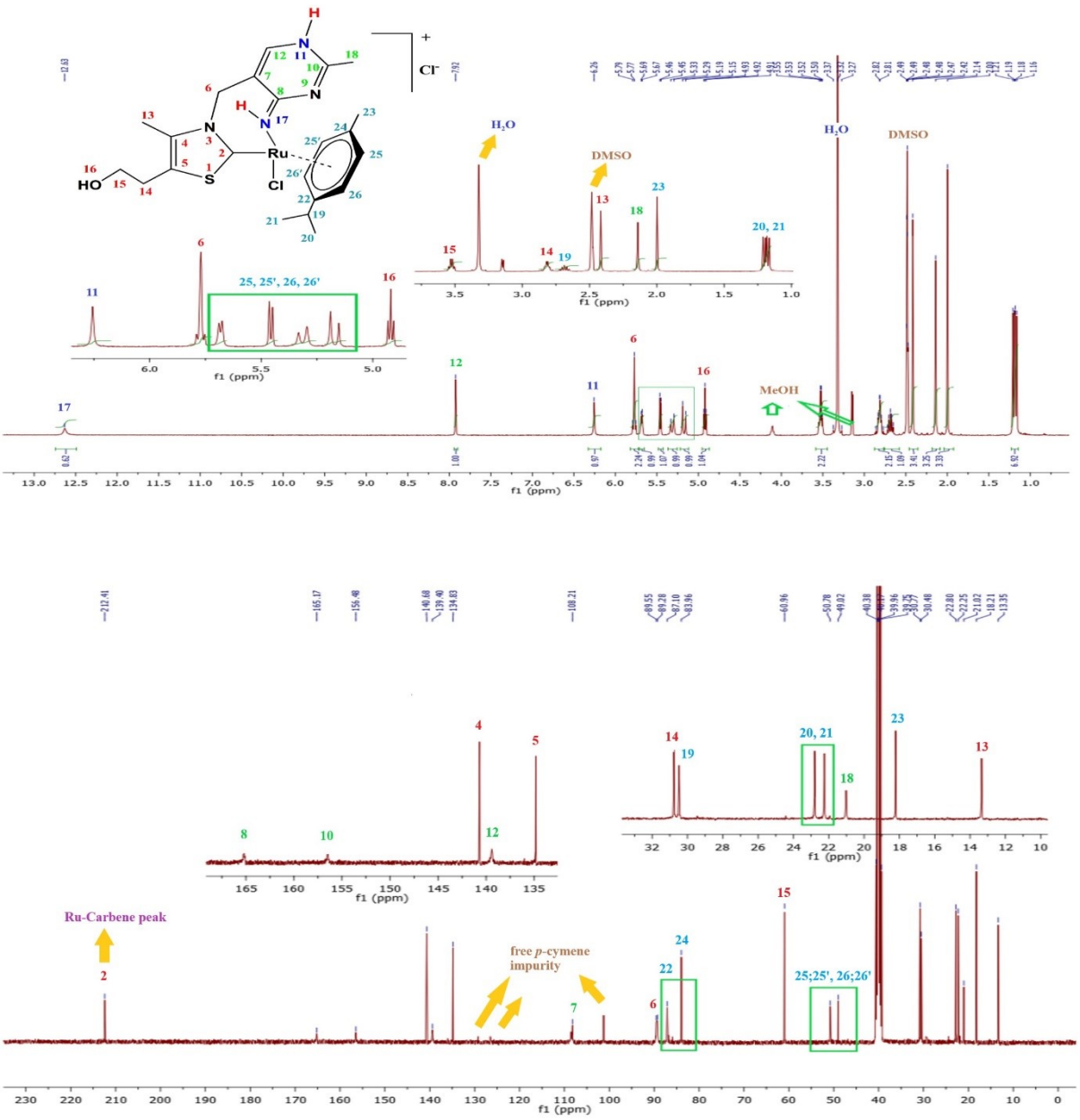

Figure S1. ^{1}H and ^{13}C NMR spectra of (**2**) complex in d^{6}-DMSO

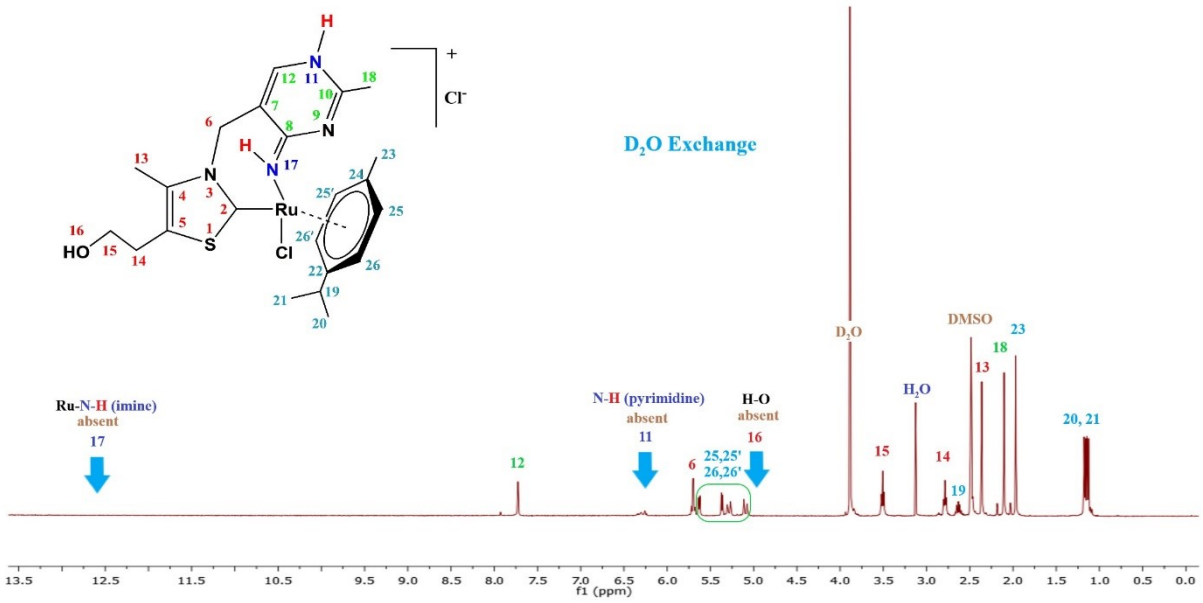

Figure S2. D_2O exchange ^{1}H-NMR spectra of (**2**) complex in *d*^{6}-DMSO

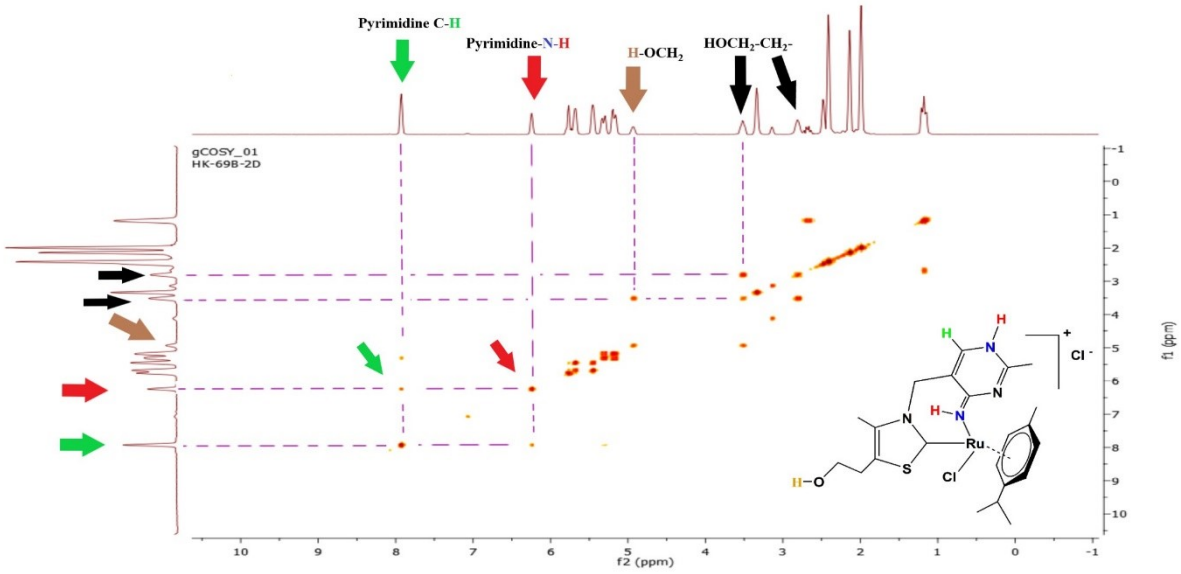

Figure S3. 1D ^{1}H (top) and ^{1}H 2D COSY (left) NMR spectra of the (**2**) in *d*^{6}-DMSO

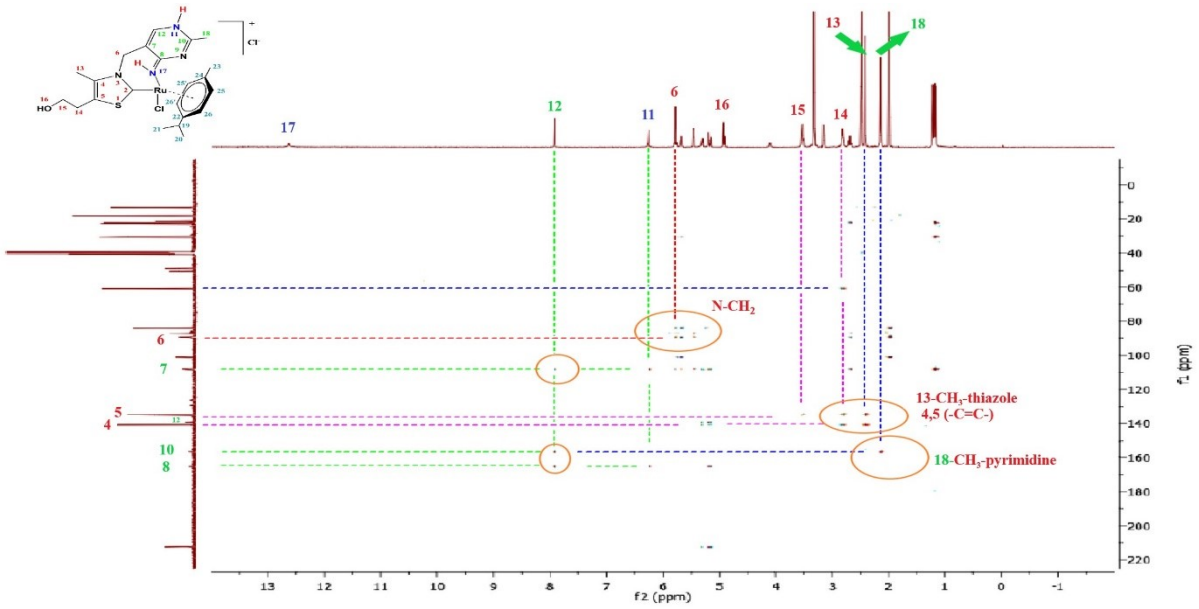

Figure S4. 1D ^{1}H (top) and ^{13}C 2D HMBC (left) NMR {^{1}H-^{13}C} spectra of (**2**) complex in *d*^{6}-DMSO

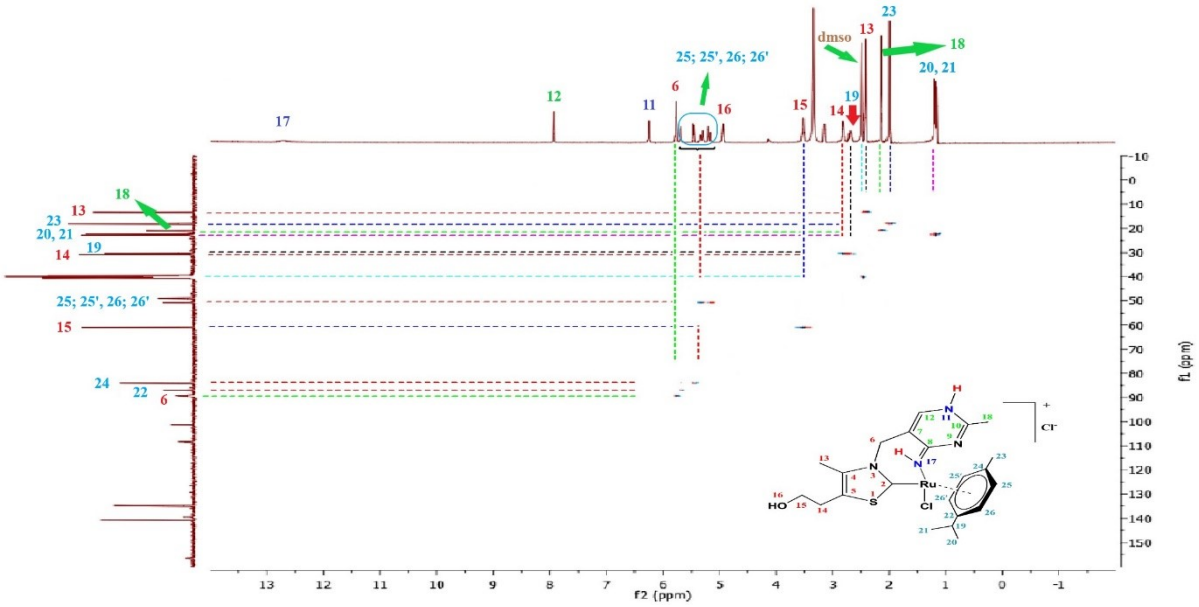

Figure S5. 1D ^{1}H (top) and ^{13}C 2D HSQC (left) NMR {^{1}H-^{13}C} spectra of (**2**) complex in *d*^{6}-DMSO

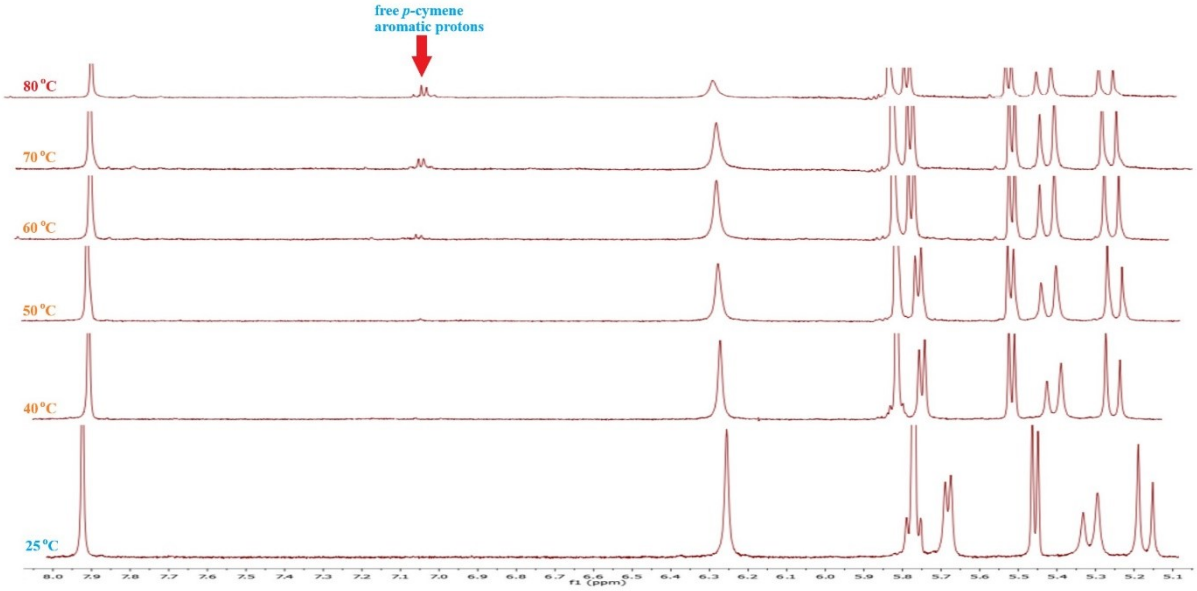

Figure S6. ^{1}H NMR spectra of (**2**) at different temperatures in d^{6}-DMSO

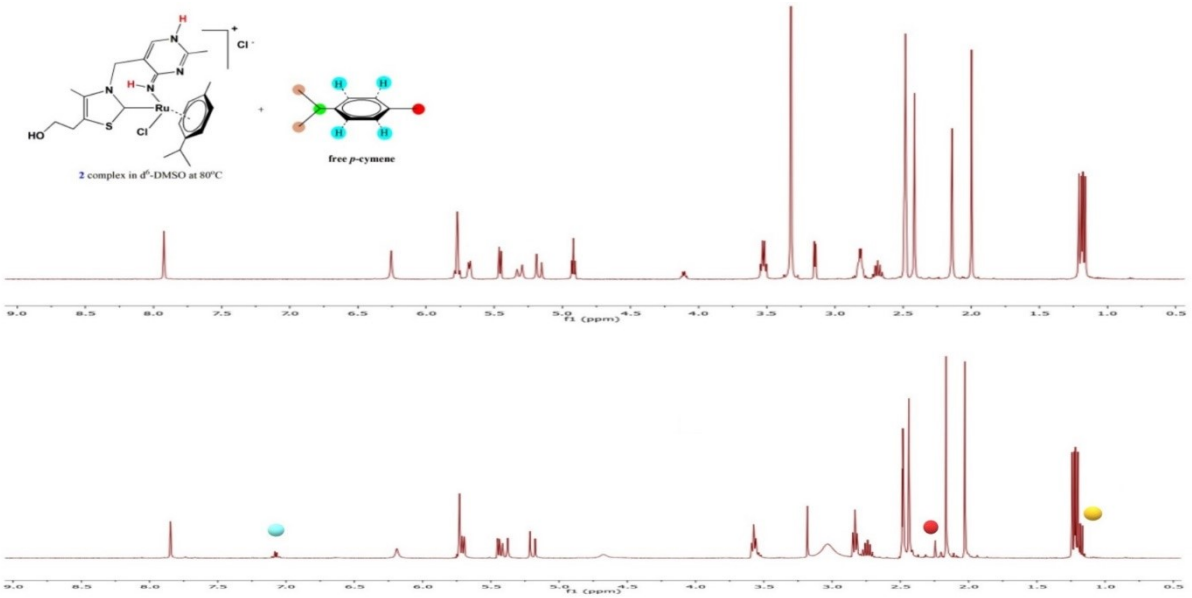

Figure S7. ^{1}H NMR spectra of (**2**) at room temperature (top) and at 80°C (bottom) in d^{6}-DMSO

Synthesis of [(p-cymene)RuCl(κ² C,N-{C_{NHC}-NH})]$^{+}PF_6^{-}$ (3)

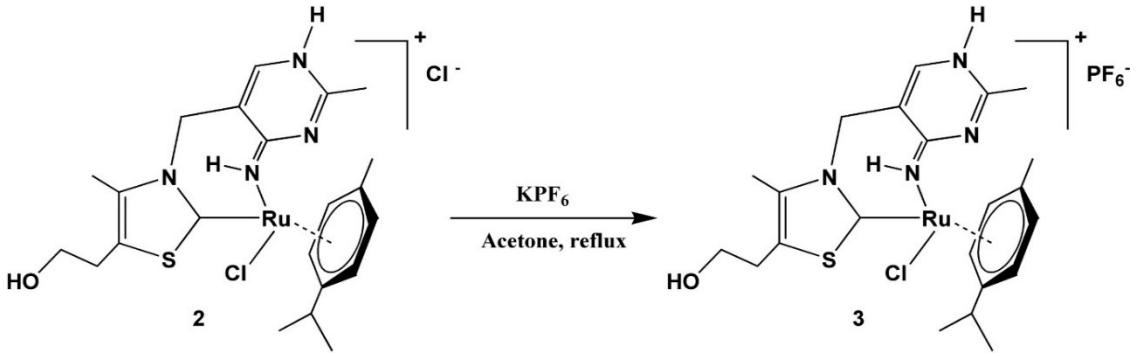

A mixture of **2** (200 mg; 0.35 mmol), KPF_6 (64.4 mg; 0.35 mmol) and 10.0 mL acetone was refluxed for 4 hours and cooled to RT. Then mixture was filtered and Et_2O was added to the filtrate to obtain red-brown crystals of **3** (204,7 mg, 86%), mp > 298 °C (decompose). Elemental analysis (%): calcd for $C_{22}H_{30}ClN_4OF_6PSRu$: C 38.9, H 4.5, N 8.2%. Found: C 38.6, H 4.6, N 8.1 ^{1}H NMR (400 MHz; d_6-DMSO): δ = 1.17 (d, J = 6.80 Hz, 3H, CH_3)$_2$CH $_{cym}$), 1.20 (d, J = 6.80 Hz, 3H, CH_3)$_2$CH $_{cym}$), 2.00 (s, 3H, CH_3 $_{cym}$), 2.13 (s, 3H, CH_3 $_{pym}$), 2.41 (s, 3H, CH_3 $_{thiaz}$), 2.65-2.72 (m, 1H, CH$_3$)$_2$CH $_{cym}$), 2.80-2.83 (m, 2H, CH_2CH$_2$-OH), 3.53 (q, J = 5.60 Hz,2H, CH$_2$CH_2-OH), 4.86 (t, J = 5.20 Hz,1H, HO-CH$_2$CH$_2$), 5.13 (d, J = 14.8 Hz, 1H, Ar-H cym), 5.32 (d, J = 15.2 Hz, 1H, Ar-H $_{cym}$), 5.45 (d, J = 6.0 Hz, 1H, Ar-H $_{cym}$), 5.68 (d, J = 5.6 Hz, 1H, Ar-H $_{cym}$), 5.77 (d$_{(distorted)}$, 2H, N-CH_2), 6.32 (br s, 1H, NH $_{pym}$), 7.88 (s, 1H, Ar-CH $_{pym}$), 12.15 (br s,1H, NH $_{imino}$). ^{13}C NMR (100,56 MHz; d_6-DMSO): δ = 13.3 (CH$_3$ $_{thiaz}$), 18.2 (CH$_3$ $_{cym}$), 21.1 (CH$_3$ $_{pym}$), 22.2, 22.8 (CH$_3$)$_2$CH $_{cym}$), 30.5 (CH$_3$)$_2C$H $_{cym}$), 30.8 (-CH$_2$CH$_2$-OH), 61.0 (-CH$_2C$H$_2$-OH), 49.0, 50.8 (Ar-CH $_{cym}$), 83.9, 87.1 (Ar-C $_{cym}$), 89.4 (N-CH$_2$), 108.3 (C $_{pym}$), 139.4 (CH $_{pym}$), 134.9, 140.6 (-C=C $_{thiaz}$), 156.5 (C $_{pym}$), 165.1 (C $_{pym}$), 212.4 (C_{NSHC}). ^{19}F NMR (376.50 MHz, d_6-DMSO): δ = -70.2 (d, J_{P-F} = 709.0 Hz, PF_6^-). ESI-HRMS: Calcd for $C_{22}H_{30}RuClN_4OS$ $[M]^+$ 535.088, $[M+2H]^+$ = found 535.138, 537.680.

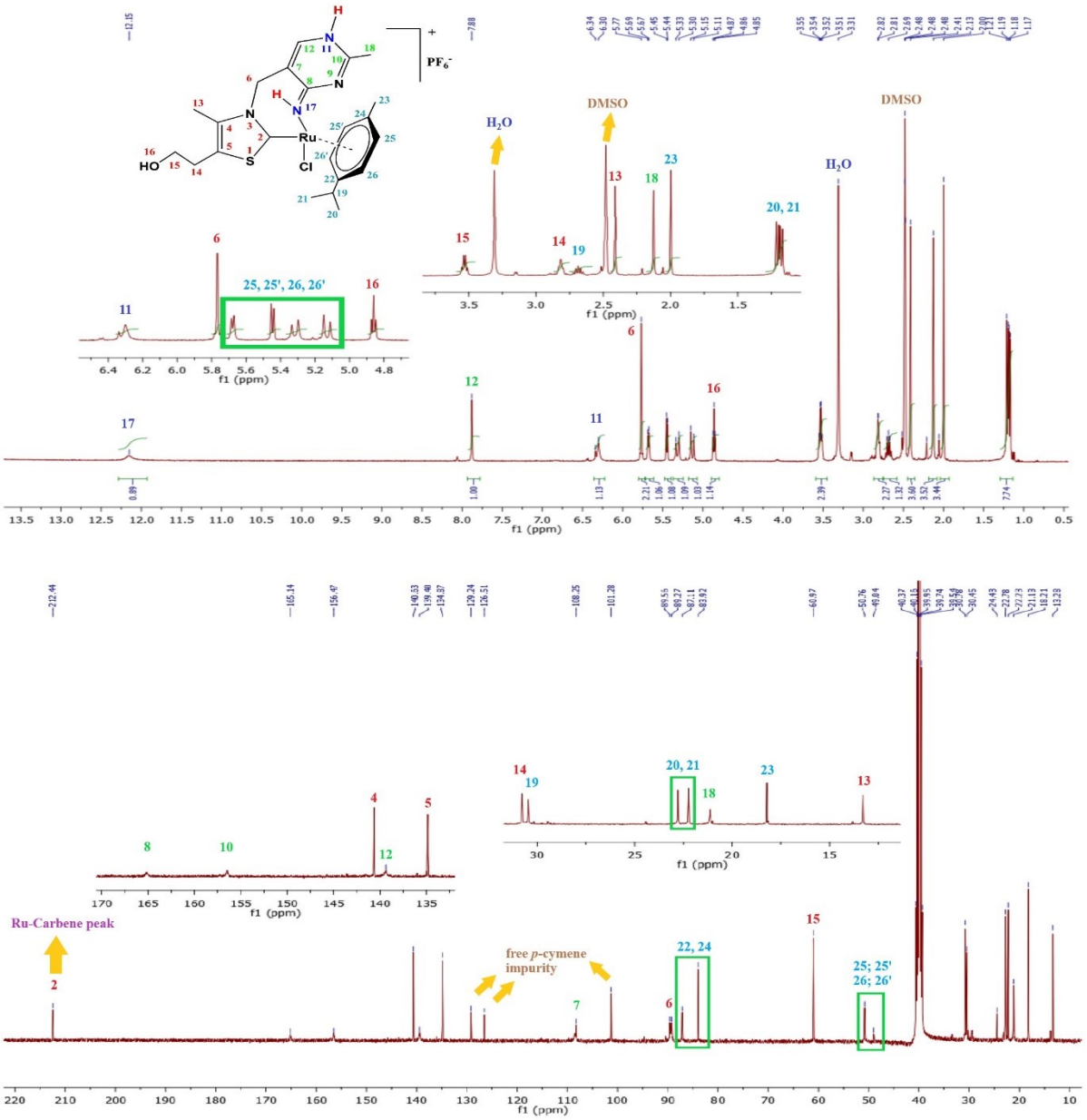

Figure S8. ^{1}H and ^{13}C NMR spectra of (**3**) complex in d^{6}-DMSO

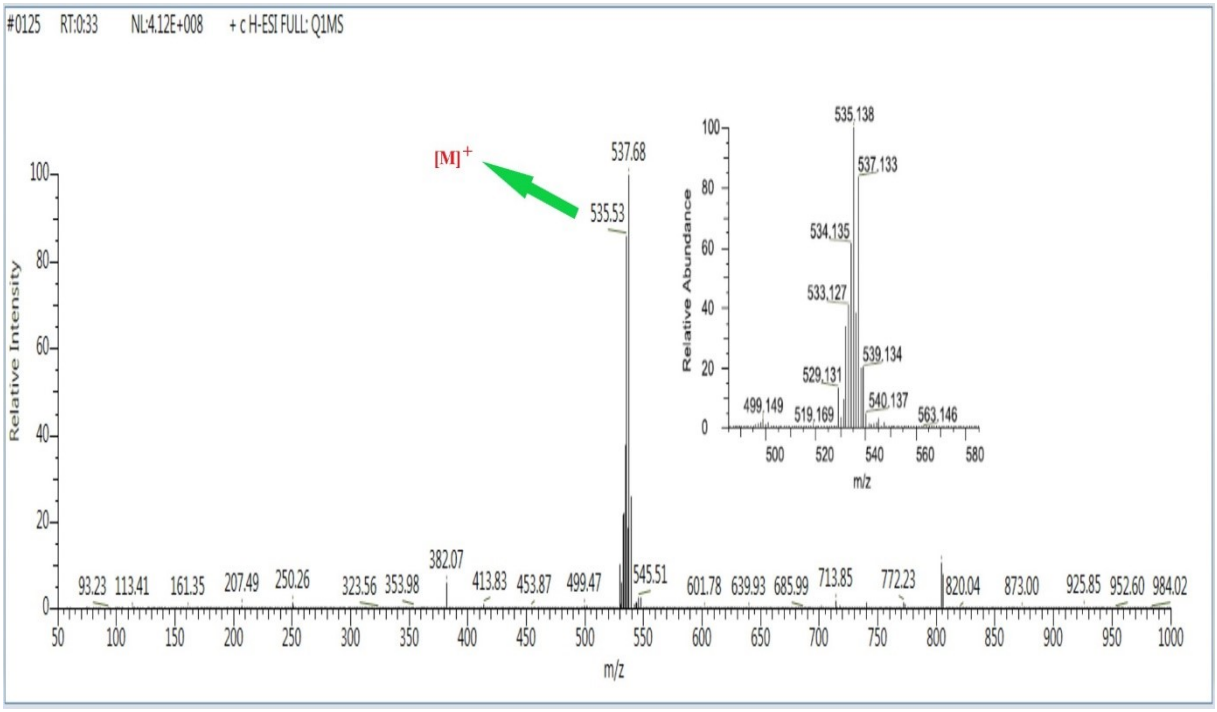

Figure S9. HR-ESI-MS spectra of (**3**) complex

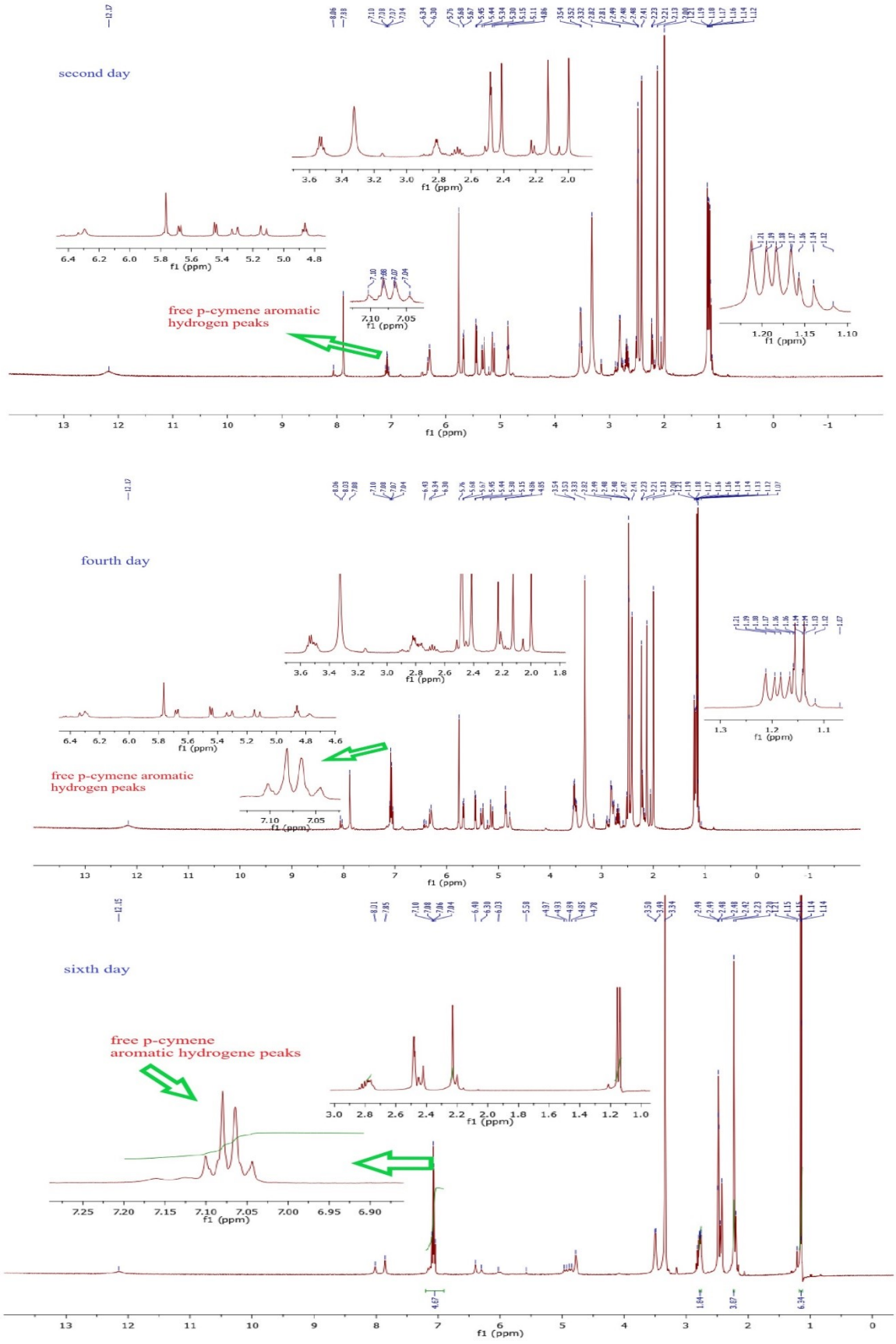

Figure S10. ^{1}H NMR spectra of (**3**) at taken by keeping it in DMSO-d^{6} solution at RT for 2, 4 and 6 days

Synthesis of [(py)$_3$RuCl(κ^2 C,N-{C$_{NHC}$-NH})]$^+$PF$_6^-$ (4)

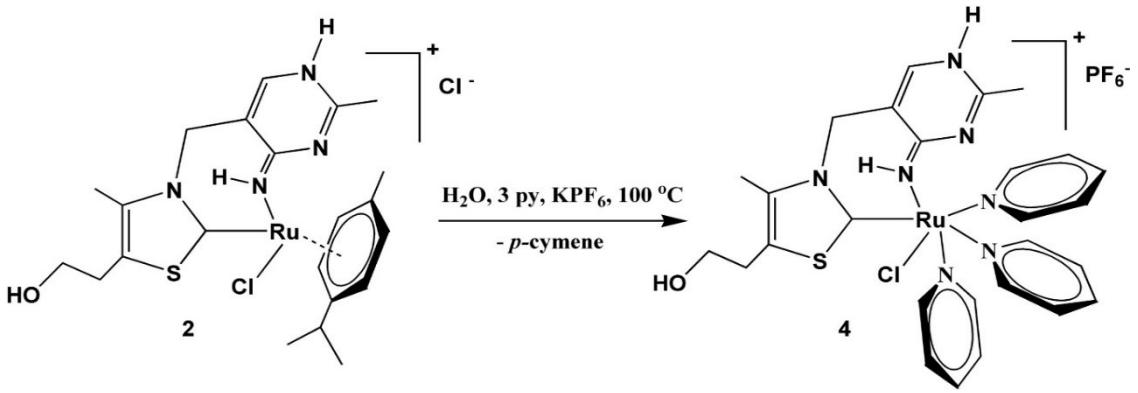

A mixture of **2** (200 mg; 0.35 mmol), pyridine (36.0 μL; 1.06 mmol), KPF_6 (64.4 mg, 0.35 mmol) and 3.0 mL H_2O was heated at 100 °C for 24 hours. At the end of the period, the water was distilled in vacuo. The remaining solid was washed with Et_2O, the chilled methanol (5 mL) was added and filtered through a celite-cannula system. The volume of the solution was reduced and diffusion of Et_2O into a saturated MeOH solution yielded yellow-green crystals, suitable for X-ray diffraction study. The solid (211.9 mg, 86%), mp > 236°C (decompose). Elemental analysis (%): calcd for $C_{27}H_{31}ClN_7OF_6PSRu$: C 41.4, H 4.0, N 12.5%. Found: C 41.2, H 4.3, N 12.4. ^{1}H NMR (400 MHz; *d*$_6$-DMSO): δ = 2.08 (s, 3H, C*H*$_{3\ pym}$), 2.37 (s, 3H, C*H*$_{3\ thiaz}$), 2.75 (t, *J* = 6.00 Hz, 2H, C*H*$_2$CH$_2$-OH), 3.49 (q, *J* = 6.00 Hz, 2H, CH$_2$C*H*$_2$-OH), 4.45 (br d, *J* = 62.8 Hz, N-C*H*$_2$), 4.71 (t, *J* = 5.20 Hz, 1H, *H*O-CH$_2$CH$_2$), 7.05 (br s, 1H, N*H*$_{pym}$), 7.34 (t, *J* = 7.20 Hz, 6H, C*H*-$_{py}$), 7.64 (s, 1H, C*H*$_{pym}$), 7.84 (t, *J* = 7.60 Hz, 3H, C*H*$_{py}$), 8.20 (d, *J* = 4.80 Hz, 6H, C*H*$_{py}$), 11.88 (br s, 1H, N*H*$_{imino}$). ^{13}C NMR (100,56 MHz; *d*$_6$-DMSO): δ = 13.9 (*C*H$_{3\ thiaz}$), 21.1 (*C*H$_{3\ pym}$), 30.9 (-*C*H$_2$CH$_2$-OH), 61.2 (-*C*H$_2$CH$_2$-OH), 46.9 (N-*C*H$_2$), 108.7 (*C*$_{pym}$), 124.7 (*C*H$_{py}$), 129.5 (*C*H$_{py}$), 136.6 (-*C*=*C*$_{thiaz}$), 138.4 (*C*H$_{pym}$), 141.5 (-*C*=*C*$_{thiaz}$), 155.0 (*C*$_{pym}$), 156.6 (*C*H$_{py}$), 167.7 (*C*$_{pym}$), 226.1 (*C*$_{NSHC}$). ^{19}F NMR (376.50 MHz, *d*$_6$-DMSO): δ = -70.2 (d, $J_{P\text{-}F}$ = 711.96 Hz).

Figure S11. ^{1}H and ^{13}C NMR spectra of (**4**) complex

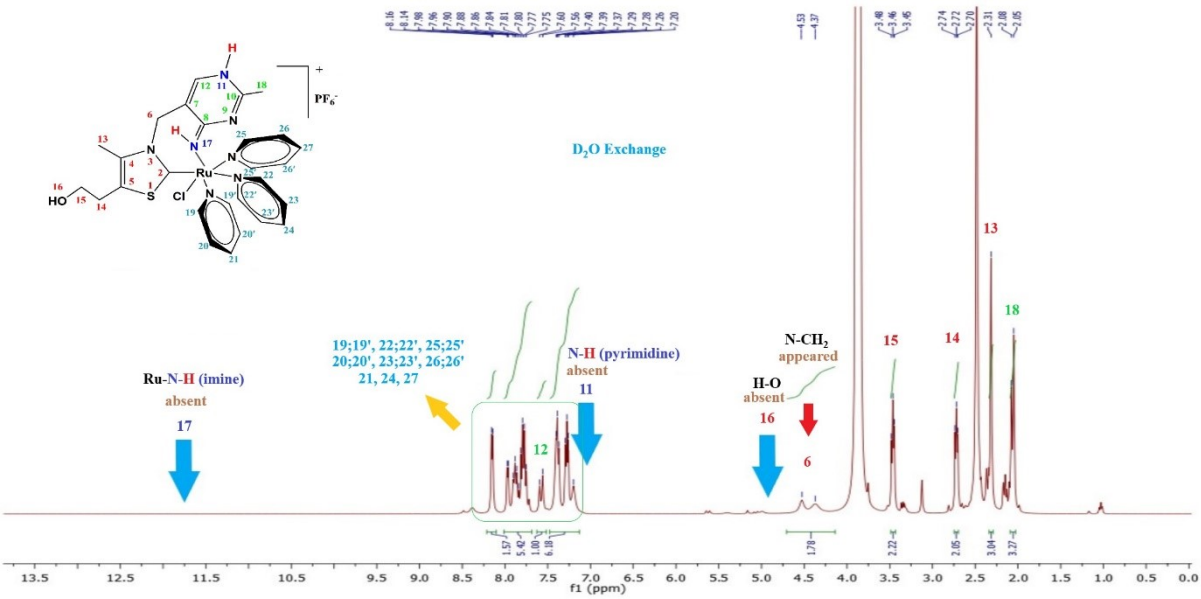

Figure S12. D_2O exchange ^{1}H-NMR spectra of (**4**) complex in *d*^{6}-DMSO

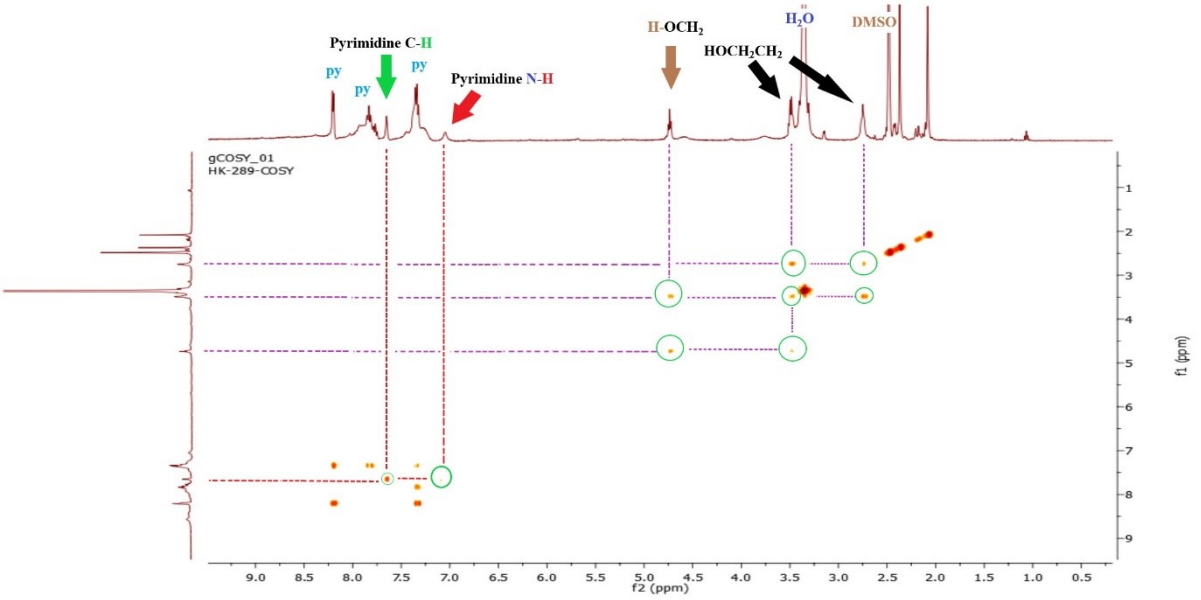

Figure S13. 1D ^{1}H (top) and ^{1}H 2D COSY (left) NMR spectra of the (**4**) in *d*^{6}-DMSO

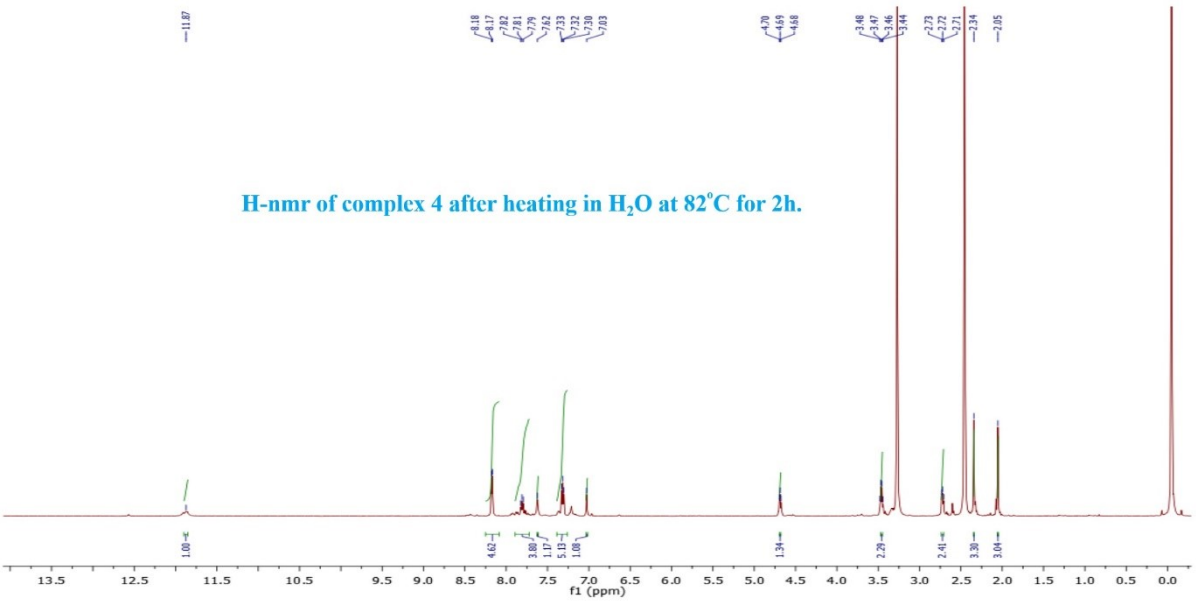

Figure S14. ^{1}H-NMR spectra of (**4**) complex in d^{6}-DMSO after heating in H_2O at 82°C for 2h.

X-ray crystallography

X-ray diffraction data for **2** were collected on a STOE IPDS II diffractometer, while crystallographic measurements for **4** were carried out on a Bruker D8 QUEST diffractometer. Structure solution and refinement were carried out using SHELXT-2018 [1] and SHELXL-2019 [2], respectively. All H atoms were located in difference maps and then treated as riding atoms, fixing the bond lengths at 0.82, 0.86, 0.93, 0.98, 0.97 and 0.96 Å for OH, NH, aromatic CH, methine CH, CH_2 and CH_3 atoms, respectively. The displacement parameters of the H atoms were fixed at $U_{iso}(H) = 1.2U_{eq}$ ($1.5U_{eq}$ for OH and CH_3) of their parent atoms. The ethanol group in **2** was disordered over two positions, and the refined site-occupancy factors of the disordered atoms are 0.501(5)% for the major position and 0.499(5)% for the minor position, respectively. For **2**; Data collection: XAREA [3], cell refinement: X-AREA, data reduction: X-RED32.[3] For **4**; Data collection: APEX2 [4], cell refinement: SAINT [4], data reduction: SAINT. Crystal data, data collection and structure refinement details are given in Table S1. Molecular graphics were created by using OLEX2.[5]

Structural description

The cationic complex, **2** consists of a bidentate (κ^2-*C,N*) ligand with an Ru(II) metal center, one *p*-cymene ligand and a chloride ligand. In the mononuclear cationic complex, the metal center is stereogenic. The complex adopts the familiar pseudo-octahedral three-legged piano-stool geometry that is common for Ru(II) η^6-arene structures, with Ru(II) π-bonded to the *p*-cymene ligand. Ru(II) ion is also coordinated to a monodentate chloride ligand and the bidentate (κ^2-*C,N*) ligand *via N,C* atoms, which constitute the three legs of the piano stool. However, the geometry around the metal atom can be considered as a tetrahedron, defining the linkage to the hydrocarbon as a single bond. Describing Cg as the centroid of the *p*-cymene ring, the Ru─Cg distance is 1.7199(14) Å, which is somewhat longer compared to that of η^6-arene complex analogues [6-8], while the Cl1─Ru1─Cg, N1─Ru1─Cg and C1─Ru1─Cg angles are 124.59(6), 128.54(9) and 129.61(11)°, respectively. The Cl1─Ru1─N1, Cl1─Ru1─C1 and N1─Ru1─C1 angles are smaller than the ideal tetrahedral angle (109.47°), which is compensated by the extending of the Cg─Ru─*L* (L is Cl1, N1 or C1) angles. The ruthenium atom is π-bonded to the *p*-cymene ring with an average Ru─C bond distance of 2.226 Å. The Ru1─Cl1, Ru1─N1 and Ru1─C1 bond distances are 2.4197(11), 2.113(3) and 2.033(3) Å, respectively. All the geometric parameters are comparable with those of other Ru(II)-arene complexes with the same coordination sphere. [6-12] The pyrimidine ring is planar with a root mean square deviation of 0.0247 Å, and the C9─N3─C10 angle is 119.9(3)°.

The asymmetric unit of the compound, **4** contains a discrete complex cation and a hexafluorophosphate anion. The cationic moiety includes the same (κ^2-*C,N*) ligand with an Ru(II) metal center, three pyridine ligands and a chloride ligand. The Ru(II) atom is coordinated in a distorted octahedral geometry by three nitrogen atoms of the pyridine ligands in mer-position, a nitrogen and a carbenic carbon atoms of the bidentate (κ^2-*C,N*) ligand, and a chloride ion. The carbenic carbon and chloride ligand in the cation adopt a *trans* arrangement with a Cl1─Ru1─C1 bond angle of 173.65(15)°. It is noteworthy that the N1─Ru1─C1 bite angle is larger by roughly 3° than the corresponding one in **2**. The Ru1─C1 bond length is 1.970(5) Å, as the Ru─N distances change from 2.084(4) to 2.114(4) Å. The bond distances and angles resemble those of analogous complexes reported in the literature [13-16] though the relatively long Ru─Cl bond distance of 2.5187(14) Å is remarkable. This bond distance was somewhat longer, presumably due to the considerable *trans* influence exerted by the highly σ-donating NSHC moiety. The pyrimidine ring is planar with a root mean square deviation of 0.0108 Å, and the angle subtended at the N3 atom is 119.9(5)°.

Table S1. Crystal data and structure refinement parameters for **2** and **4**.

Parameters	**2**	**4**
CCDC depository	2233948	2321199
Color/shape	Yellow/prism	Yellow/block
Chemical formula	$[RuCl(C_{10}H_{14})(C_{12}H_{16}N_4OS)]^+ \cdot Cl^-$	$[RuCl(C_5H_5N)_3(C_{12}H_{16}N_4OS)]^+ \cdot PF_6^-$
Formula weight	570.53	783.14
Temperature (K)	296(2)	296(2)
Wavelength (Å)	0.71073 Mo Kα	0.71073 Mo Kα
Crystal system	Monoclinic	Monoclinic
Space group	*I*2/*a* (No. 15)	$P2_1/c$ (No. 14)
Unit cell parameters		
a, *b*, *c* (Å)	17.852(5), 18.543(4), 16.781(5)	11.4006(15), 18.081(2), 15.713(2)
α, *β*, *γ* (°)	90, 116.80(2), 90	90, 98.410(4), 90
Volume (Å^3)	4958(2)	3204.2(7)
Z	8	4
$D_{calc.}$ (g/cm^3)	1.529	1.623
μ (mm^{-1})	0.954	0.758
Absorption correction	Integration	Multi-scan
$T_{min.}$, $T_{max.}$	0.6551, 0.9288	0.4909, 0.7456
F_{000}	2336	1584
Crystal size (mm^3)	0.79 × 0.23 × 0.12	0.09 × 0.05 × 0.04
Diffractometer/measurement method	STOE IPDS II/ω scan	Bruker D8 QUEST/φ and ω scan
Index ranges	$-22 \le h \le 22$, $-23 \le k \le 22$, $-19 \le l \le 20$	$-13 \le h \le 13$, $-21 \le k \le 21$, $-18 \le l \le 18$
θ range for data collection (°)	$1.685 \le \theta \le 26.339$	$1.806 \le \theta \le 25.048$
Reflections collected	35515	104463
Independent/observed reflections	5015/3229	5683/4878
$R_{int.}$	0.0905	0.0735
Refinement method	Full-matrix least-squares on F^2	Full-matrix least-squares on F^2
Data/restraints/parameters	5015/67/308	5683/0/409
Goodness-of-fit on F^2	0.845	1.177
Final *R* indices [$I > 2\sigma(I)$]	$R_1 = 0.0330$, $wR_2 = 0.0598$	$R_1 = 0.0549$, $wR_2 = 0.1276$
R indices (all data)	$R_1 = 0.0718$, $wR_2 = 0.0664$	$R_1 = 0.0657$, $wR_2 = 0.1334$
$\Delta\rho_{max.}$, $\Delta\rho_{min.}$ (e/Å^3)	0.44, −0.38	1.62, −0.62

Table S2. Selected geometric parameters for **2** and **4**.

Parameters	2	Parameters	4
Bond lengths (Å)			
Ru1─Cg	1.7199(14)	Ru1─Cl1	2.5187(14)
Ru1─Cl1	2.4197(11)	Ru1─N1	2.084(4)
Ru1─N1	2.113(3)	Ru1─N5	2.091(4)
Ru1─C1	2.033(3)	Ru1─N6	2.114(4)
Ru1─C_{arene}	2.189(3)-2.287(3)	Ru1─N7	2.107(4)
N1─C12	1.309(4)	Ru1─C1	1.970(5)
N2─C10	1.304(4)	N1─C12	1.293(6)
N2─C12	1.393(4)	N2─C10	1.294(7)
N3─C9	1.367(4)	N2─C12	1.388(7)
N3─C10	1.346(4)	N3─C9	1.362(8)
N4─C1	1.341(4)	N3─C10	1.350(8)
N4─C5	1.415(4)	N4─C1	1.369(7)
N4─C7	1.490(4)	N4─C5	1.407(7)
S1─C1	1.712(3)	N4─C7	1.476(7)
S1─C2	1.729(4)	S1─C1	1.730(6)
		S1─C2	1.725(6)
Bond angles (°)			
Cl1─Ru1─N1	84.73(8)	C1─Ru1─N1	90.48(19)
Cl1─Ru1─C1	87.13(9)	C1─Ru1─N5	92.3(2)
Cl1─Ru1─Cg	124.59(6)	N1─Ru1─N5	96.86(17)
Cl1─Ru1─C_{arene}	86.99(10)-160.28(9)	C1─Ru1─N7	91.7(2)
N1─Ru1─C1	87.78(12)	N1─Ru1─N7	86.24(17)
N1─Ru1─Cg	128.54(9)	N5─Ru1─N7	174.95(16)
N1─Ru1─C_{arene}	91.16(12)-160.72(13)	C1─Ru1─N6	96.77(19)
C1─Ru1─Cg	129.61(11)	N1─Ru1─N6	172.03(17)
C1─Ru1─C_{arene}	90.73(13)-164.45(12)	N5─Ru1─N6	86.20(17)
C1─S1─C2	93.82(17)	N7─Ru1─N6	90.22(17)
N1─C12─N2	117.3(3)	C1─Ru1─Cl1	173.65(15)
N1─C12─C8	123.8(3)	N1─Ru1─Cl1	83.37(13)
N2─C10─N3	123.2(3)	N5─Ru1─Cl1	90.04(13)
C9─N3─C10	119.9(3)	N7─Ru1─Cl1	86.34(12)
C1─N4─C5	117.1(3)	N6─Ru1─Cl1	89.28(12)
C1─N4─C7	120.2(3)	C1─S1─C2	94.9(3)
C5─N4─C7	122.7(3)	N1─C12─N2	119.1(5)
N4─C1─S1	108.0(2)	N1─C12─C8	122.1(5)
		N2─C10─N3	123.2(6)
		C9─N3─C10	119.9(5)
		C1─N4─C5	117.1(5)
		C1─N4─C7	122.2(4)
		C5─N4─C7	119.6(5)
		N4─C1─S1	105.7(4)

Note: Cg represents the centroid of the arene ring.

Computational procedure

Quantum-chemical computations were carried out with the Gauss View 5 [17] molecular visualization program and the Gaussian 09 program package.[18] The molecular structures were optimized using HSEH1PBE density functional method [19-22] and SDD basis set.[23,24] The calculated vibrational frequencies ascertained that the structures were stable (no imaginary frequencies).

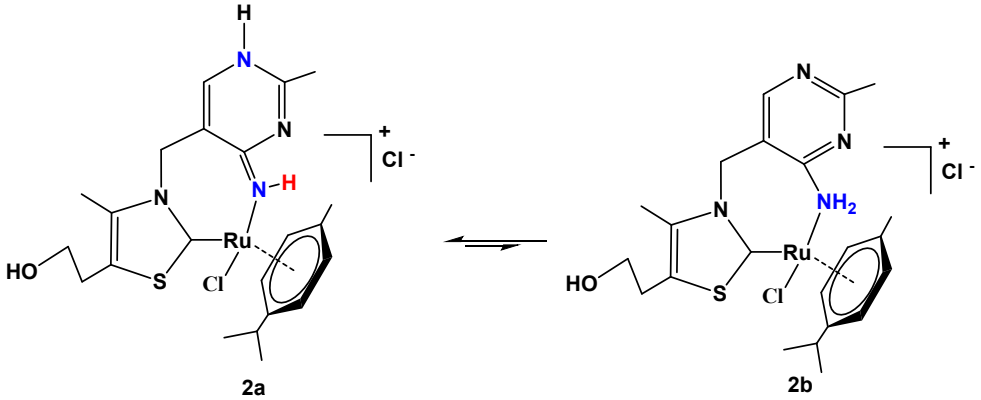

According to the calculated total energies, the relative order of stability of the complexes is **2a** > **2b**.

Table S3. Energies for the optimized structures.

Compound	E_{298K}[a] **(Hartree)**	H_{298K}[a] **(Hartree)**	G_{298K}[a] **(Hartree)**
2a	-2561,802579	-2561,767652	-2561,871789
2b	-2561,782268	-2561,747616	-2561,849103
Δ*E* (kj mol^{-1})	53.35	52.59	59.58

[a] standard conditions T = 298.15 K and p = 1 atm.

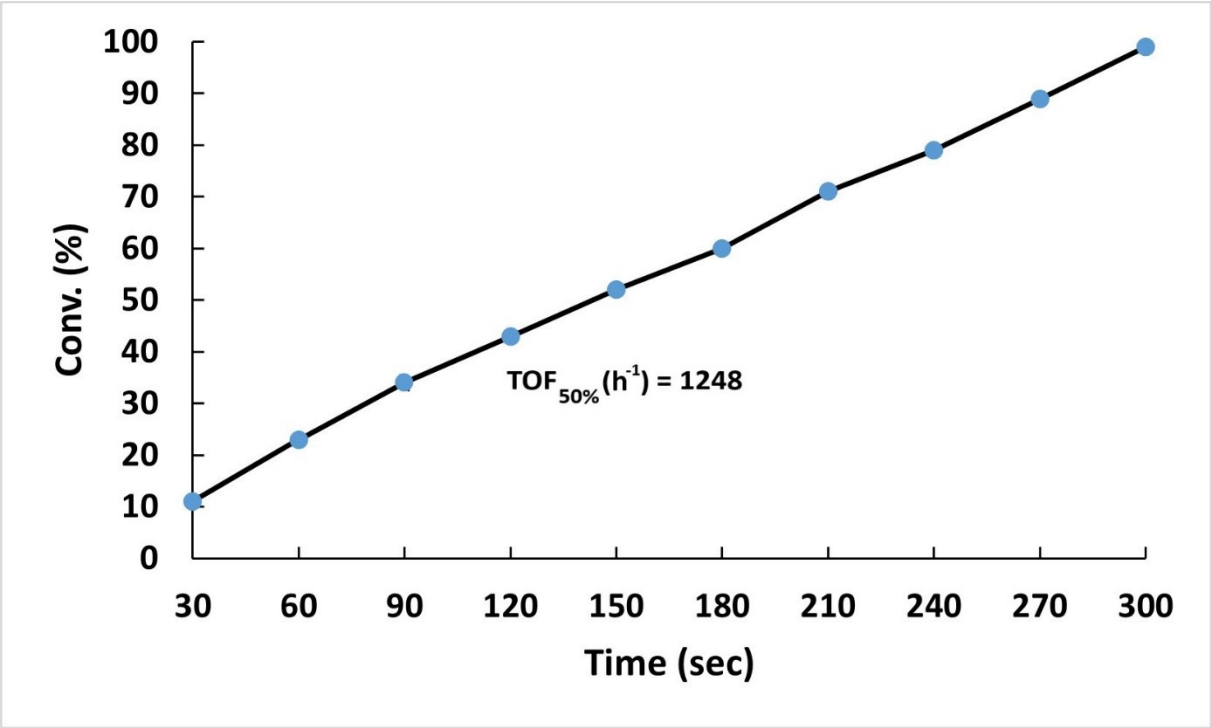

Figure S15. Kinetic profile of the catalytic TH of acetophenone to acetophenol applying the complex **4** at 82 °C with HCO_2H/NEt_3 buffer (5/2) in H_2O at 0.01 mmol catalyst loading and turnover frequencies (TOF = mole of acetophenone per mole of Ru per hour at 50% conversion)

References

1 G. M. Sheldrick, *Acta Crystallogr. Sect.*, A 2015, **71**, 3−8.

2 G. M. Sheldrick, *Acta Crystallogr. Sect. C*, 2015, **71**, 3−8.

3 Stoe & Cie (2002). X-AREA Version 1.18 and X-RED32 Version 1.04. Stoe & Cie GmbH, Darmstadt, Germany.

4 Bruker (2013). APEX2 and SAINT. Bruker AXS Inc., Madison, Wisconsin, USA.

5 O. V. Dolomanov, L. J. Bourhis, R. J. Gildea, J. A. K. Howard and H. Puschmann, *J. Appl. Crystallogr.*, 2009, **42**, 339−341.

6 J. G. Malecki, M. Jaworska, R. Kruszynski and J. Klak, *Polyhedron*, 2005, **24**, 3012-3021.

7 D. Aguilar, R. Bielsa, T. Soler and E. P. Urriolabeitia, *Organometallics,* 2011, **30**, 642-648.

8 A. G. Nair, R. T. McBurney, D. B. Walker, M. J. Page, M. R. D. Gatus, M. Bhadbhade and B. A. Messerle, *Dalton Trans.,* 2016, **45**, 14335-14342.

9 S. Attar, J. H. Nelson, J. Fischer, A.de Cian, J.-P. Sutter and M. Pfeffer, *Organometallics,* 1995, **14**, 4559-4569.

10 H. C. L. Abbenhuis, M. Pfeffer, J.-P. Sutter, A. de Cian, J. Fischer, H. L. Ji and J. H. Nelson, *Organometallics,* 1993, **12**, 4464-4472.

11 N. Gül and J. H. Nelson, *Polyhedron,* 1999, **18**, 1835-1843.

12 N. Gül and J. H. Nelson, *Organometallics,* 1999, **18**, 709-725.

13 M. Dakkach, X. Fontrodona, T. Parella, A. Atlamsani, I. Romero and M. Rodriguez, *Adv. Synth. Catal.,* 2011, **353**, 231-238.

14 M. Dakkach, A. Atlamsani, T. Parella, X. Fontrodona, I. Romero and M. Rodriguez, *Inorg. Chem.,* 2013, **52**, 5077-5087.

15 H.-J. Liu, M. Gill-Sepulcre, L. Francas, P. Nolis, T. Parella, J. Benet-Buchholz, X. Fontrodona, J. Garcia-Anton, N. Romero, A. Llobet, L. Escriche, R. Bofill and X. Sala, *Dalton Trans.,* 2017, **46**, 2829-2843.

16 S. Gonell, E. A. Assaf, K. D. Duffee, C. K. Schauer and A. J. M. Miller, *J. Am. Chem. Soc.,* 2020, **142**, 8980-8999.

17 R. Dennington, T. Keith and J. Millam, GaussView, Version 5.0, Semichem Inc., Shawnee Mission, KS, 2009.

18 M. J. Frisch, G. W. Trucks, H. B. Schlegel, G. E. Scuseria, M. A. Robb, J. R. Cheeseman, G. Scalmani, V. Barone, G. A. Petersson, H. Nakatsuji, X. Li, M. Caricato, A. Marenich, J.

Bloino, B. G. Janesko, R. Gomperts, B. Mennucci, H. P. Hratchian, J. V. Ortiz, A. F. Izmaylov, J. L. Sonnenberg, D. Williams-Young, F. Ding, F. Lipparini, F. Egidi, J. Goings, B. Peng, A. Petrone, T. Henderson, D. Ranasinghe, V. G. Zakrzewski, J. Gao, N. Rega, G. Zheng, W. Liang, M. Hada, M. Ehara, K. Toyota, R. Fukuda, J. Hasegawa, M. Ishida, T. Nakajima, Y. Honda, O. Kitao, H. Nakai, T. Vreven, K. Throssell, J. A. Montgomery, Jr., J. E. Peralta, F. Ogliaro, M. Bearpark, J. J. Heyd, E. Brothers, K. N. Kudin, V. N. Staroverov, T. Keith, R. Kobayashi, J. Normand, K. Raghavachari, A. Rendell, J. C. Burant, S. S. Iyengar, J. Tomasi, M. Cossi, J. M. Millam, M. Klene, C. Adamo, R. Cammi, J. W. Ochterski, R. L. Martin, K. Morokuma, O. Farkas, J. B. Foresman and D. J. Fox, Gaussian 09, Revision C.01, Gaussian, Inc., Wallingford CT, 2009.

19 J. Heyd and G.E. Scuseria, *J. Chem. Phys*., 2004, **120**, 7274−7280.

20 J. Heyd and G.E. Scuseria, *J. Chem. Phys*., 2004, **121**, 1187−1192.

21 J. Heyd, J. E. Peralta, G. E. Scuseria and R. L. Martin, *J. Chem. Phys*., 2005, **123**, 1−8.

22 J. Heyd, G. E. Scuseria and M. Ernzerhof, *J. Chem. Phys*., 2006, **124**, 219906.

23 T. H. Dunning Jr. and P. J. Hay, in Modern Theoretical Chemistry, Ed. H. F. Schaefer III, Vol. 3, Plenum, New York, 1977, 1−28.

24 W. Kuechle, M. Dolg, H. Stoll and H. Preuss, *J. Chem. Phys*., 1994, **100**, 7535−7342.